Tooth Root Bending Strength of Shot-Peened Gears Made of High-Purity Steels up to the VHCF Range

Daniel Fuchs, Dr. Thomas Tobie and Prof. Karsten Stahl

Introduction

Standardized methods, like AGMA 2001-D04 (Ref. 1) or ISO 6336 (Ref. 2) for the calculation of the load carrying capacities of gears are intentionally conservative to ensure broad applicability in industrial practice. However, new applications and higher requirements often demand more detailed design calculations nowadays; for example: long operating lives in wind power gearboxes or fewer gear stages and higher speeds in e-mobility applications result in higher load cycles per tooth in a gearbox. Higher load carrying capacities in the very high cycle fatigue range (VHCF) are therefore gaining significance.

One approach to strengthen the tooth root of gears is to shot-peen the tooth root fillet. This results in higher compressive residual stresses in the tooth root area and can lead to a higher tooth root bending strength. However, a drawback is that in the VHCF range, crack initiation can often occur from below the surface at a nonmetallic inclusion. Consequently, a working hypothesis is: the higher the cleanliness, the fewer and smaller-sized the nonmetallic inclusions in the material will be, and therefore the higher the tooth root load carrying capacity of case-hardened, shot-peened gears. This working hypothesis is verified in the framework of this publication.

Brief Overview of the State of Knowledge

Higher tooth root load carrying capacities are achievable using a shot-peening process in the tooth root fillet of gears. However, a change in the crack area characteristic can occur even up to a high number of load cycles, i.e. in the VHCF range. The crack can start in the steel matrix at a nonmetallic inclusion and lead to a so-called fisheye failure.

Fisheye Failure: Crack Initiation Below the Surface at Nonmetallic Inclusions

Case-hardened, shot-peened gears can fail due to a crack initiation below the surface at a nonmetallic inclusion. This so-called fisheye failure starts in the case of MnCr- or CrNiMo-alloyed steels (e.g. 20MnCr5 or 18CrNiMo7-6) typically at two main inclusion types: oblong manganese sulfides in MnCr-alloyed steels and spherical or oblong aluminum oxides in CrNiMo-alloyed steels (Figure 1).

Load Carrying Capacity Characteristics in the VHCF Range

In rotary bending investigations at room temperature (Ref. 3), a two-step S-N-curve is observable. The first step describes the surface fatigue limit and the surface finite life fatigue strength. The crack initiation is in this case always at the surface. In the range of higher numbers of load cycles, however, the crack mechanism changes, which leads to a second step and an internal fatigue limit. The crack occurs in the internal fatigue range in the material at a nonmetallic inclusion. Failures below the surface in shot-peened standard specimens are also documented for between 10^7 and 10^9 load cycles (Refs. 4–13).

Investigations of up to $1{,}0^{10}$ load cycles, which showed such failures, have also been carried out (Refs. 14, 15). Fatigue failures in the VHCF range have been documented for bearing steels (Ref. 16), nitrocarburized specimens (Ref. 17), austempered ductile iron (ADI) (Ref. 18), dual-phase steels (Ref. 19), and welded joints (Ref. 20). Murukami et al. (Refs. 21, 22), Mughrabi (Refs. 23, 24) and Bathias (Refs. 17, 25) do not specify a second fatigue limit in the range of a higher

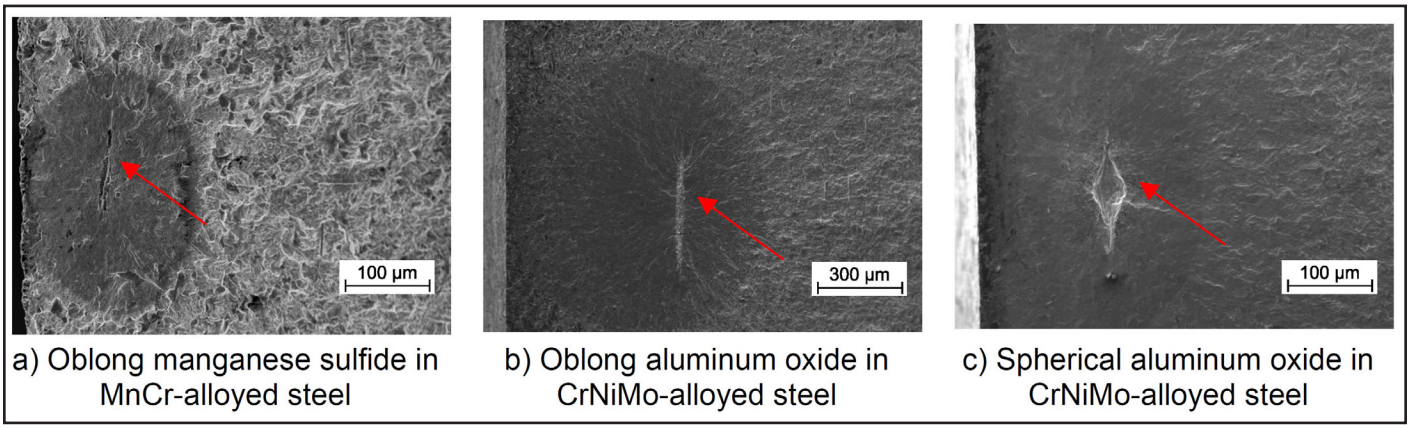

Figure 1 Typical nonmetallic inclusions in fisheye fracture surfaces of gear steels.

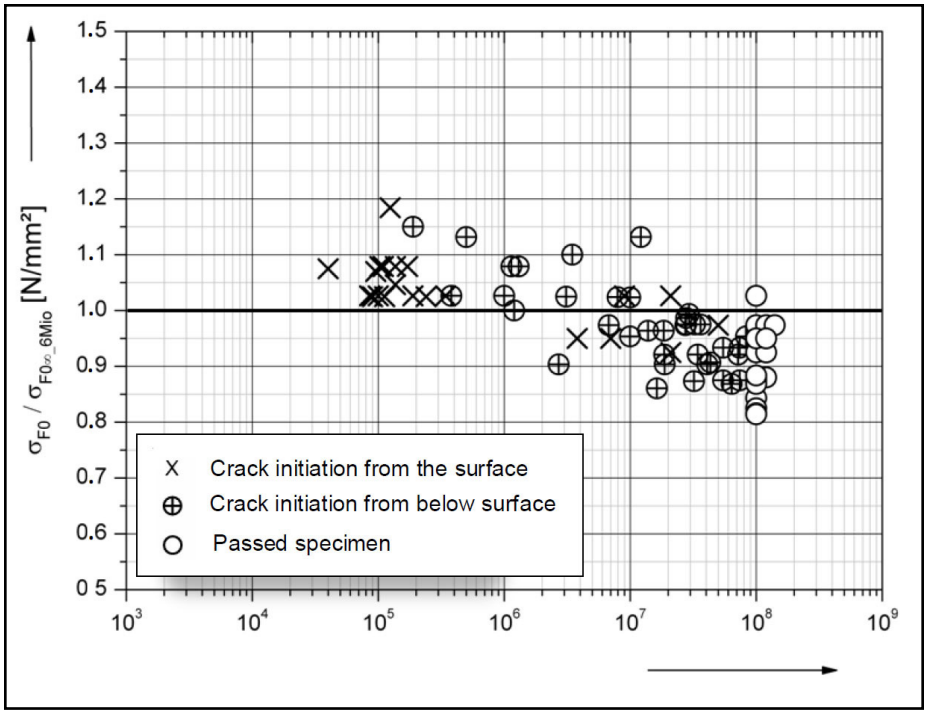

Figure 2 Summary of results of various tests with case-hardened, shot-peened gears reported in (Ref. 26, translated); (y-axis: ratio of nominal tooth root stress σ_{F0} for each test point and nominal tooth root stress for 50% failure probability at a load cycle limit of 6 million $\sigma_{F0\infty\_6Mio}$ for each variant).

Table 1 Overview of the investigated variants and properties

Variant	Material	Characterization of the heat	Casting method	Bar diameter in mm	Degree of deformation
S4	20MnCr5	Open-hearth melted	Continuous casting	105	8:1
S6		Open-hearth melted	Continuous casting	105	
S8		Electro-slag remelted (ESR)	Ingot casting	100	

Table 2 Gear data

Parameter	Symbol	Unit	Pinion	Wheel
Normal module	m_n	mm	1.5	
Tooth width	b	mm	8	
Number of teeth	z_1/z_2	-	59	61
Normal pressure angle	α_n	°	20	
Helix angle	β	°	0	
Profile shift coefficient	x	-	-0.13	1.19
Transverse contact ratio	ε_α	-	1.24	
Base diameter	d_b	mm	83.2	86.0
Pitch diameter	d	mm	88.5	91.5
Tip diameter	d_a	mm	91.5	96.0

Table 3 Shot-peening parameters (manufacturer information)

Gear size m_n in mm		**1.5**
Shot-peened area		Tooth root fillet
Size and hardness of shot	**1. step**	StD-G3, 0.40 mm, VDFI 8001, 700 HV (Cut wire, spherical)
	2. step	Glass beads, 250 – 425 µm
Shot density in %	**1. step**	1.00 – 1.25 x t 98 %
	2. step	1.75 – 2.00 x t 98 %
Intensity in mm A	**1. step**	0.23 – 0.28
	2. step	0.08 – 0.12

Table 4 Tooth root stress resulting from the load torque at the pinion according to Reference 31 under consideration of the load-dependent transverse contact ratio

Load torque in Nm	Load-dependent transverse contact ratio	Tooth root stress* (under additional consideration of the dynamic factor K_v acc. to ISO 6336 (Ref. 2) in N/mm²
130	1.30	1080
150	1.49	1213
170	1.55	1366
190	1.66	1489
210	1.69	1630
230	1.75	1773
250	1.78	1916

*Mean value over the tooth width of the tooth root stress values determined with the aid of RIKOR I (Ref. 34) and taking into account the dynamic factor KV = 1.06 acc. to ISO 6336 (Ref. 2)

number of load cycles. A steady decline is expectedeven up to 10^9–10^{10} load cycles.

In the case of shot-peened gears, studies by Stenico (Ref. 27, based on Ref. 28) and Bretl (Ref. 26, based on Ref. 29) display similar characteristics to those documented for standard specimens. The test results in Reference 26 show, foremost, failures due to subsurface crack initiation at nonmetallic inclusions up to 10^8 load cycles (Fig. 2). Bretl (Ref. 26, with experimental results internationally published in Ref. 30) also attests a second knee in the S-N curve for case-hardened, shot-peened gears, and even up to 10^8 load cycles a decrease in the endurance fatigue life. As a result, no second internal fatigue limit was determined. He states that the surface fatigue limit is primarily influenced by the residual stress state and that the slope of the S-N curve at a higher number of load cycles is mainly influenced by the degree of cleanliness. However, in Reference 26, only a limited number of investigations have been carried out on shot-peened gears up to 10^7 respectively 10^8 load cycles on the pulsator test rig.

Schurer (Ref. 31) builds on the results of Bretl (Ref. 26). In the framework of Schurer's work (with experimental results internationally published in References 32 and 33), extended experimental investigations on the pulsator and the FZG back-to-back test rig were performed regarding fisheye failures in the tooth root of case-hardened, shot-peened gears. The gears were made out of steel with different degrees of cleanliness. The limiting number of load cycles was set to $15 \cdot 10^6$ (for some test points $50 \cdot 10^6$) in the pulsator tests and $30 \cdot 10^6$ or $50 \cdot 10^6$ in the back-to-back tests. In the experimental tests even up to $50 \cdot 10^6$ load cycles, tooth root failures due to crack initiation below the surface at a nonmetallic inclusion occurred. This led to a decrease in the tooth root load carrying capacity in the very high cycle fatigue range. In addition, it was confirmed that the degree of cleanliness has a nonnegligible influence. However, due to the limited number of test points, no proper differentiation between the variants could be made. In particular, no proper differentiation could be made based on the degree of cleanliness. In Figure 3, the test results of three test variants (S4, S6, and S8) on

the pulsator test rig are shown for later comparison. The test results of Schurer (Ref. 31) on the FZG back-to-back test rig are directly given in the S-N diagrams later in the publication.

Aim of the Investigation

The aim of the investigation presented in this publication was to broaden the database of the investigations of Schurer on the FZG back-to-back test rig. On the one hand, further tests were carried out and on the other hand, the limiting number of load cycles was set at $100 \cdot 10^6$ load cycles. Three variants (S4, S6, and S8) from Reference 31 with different degrees of cleanliness were chosen. Table 1 gives an overview of the chosen variants and their properties. Further characteristics are presented below, in the section on Material and Gear Characterization. The variants are all 20MnCr5 steels but have different process routes and characteristics. In the second step, based on the broadened database, a probable correlation between the experimental results and the degree of cleanliness are checked again.

The tests were performed on a so-called FZG back-to-back test rig with a center distance of $a = 91.5$ mm. The inspection interval for the tests was $2.5 \cdot 10^6$ load cycles. Test pinion and test gear are mounted on two parallel shafts. These shafts are connected to a drive gear stage with the same gear ratio. A defined static torque is applied by twisting the load clutch on the two separate parts of the test pinion shaft. Hereby, defined weights on a load lever or a bracing device are used. For the investigations case-hardened gears with a gear size of normal module 1.5 mm were used. The gear data are given in Table 2. All gears were two-staged shot-peened in the tooth root fillet to induce high compressive residual stresses. In the first stage, cut wire was used, and in the second stage, glass bead; see Table 3.

Please note: The tooth root stress values are deliberately not shown in the later S-N curve diagrams. This is due to the nonlinear relationship between the torque applied to the pinion and the resulting nominal tooth root stress. Table 4 lists the tooth root stress valid for the respective test torque.

Table 5 Chemical composition of the test variants and threshold values according to DIN EN ISO 683-3 (Ref. 35)

Variant	Material		Chemical composition in mass-%									
			C	Mn	Cr	Ni	Mo	S	Al	Cu	P	Si
S4	20MnCr5		0.21	1.20	1.14	0.15	0.04	0.028	0.030	0.14	0.009	0.15
S6			0.18	1.25	1.07	0.22	0.06	0.012	0.023	0.09	0.012	0.26
S8			0.18	1.12	1.15	0.19	0.05	0.006	0.019	0.12	0.016	0.16
20MnCr5 acc. to (Ref. 35)		max.	0.22	1.40	1.30	–	–	0.035	–	–	0.025	0.40
		min.	0.17	1.10	1.00	–	–	–	–	–	–	–

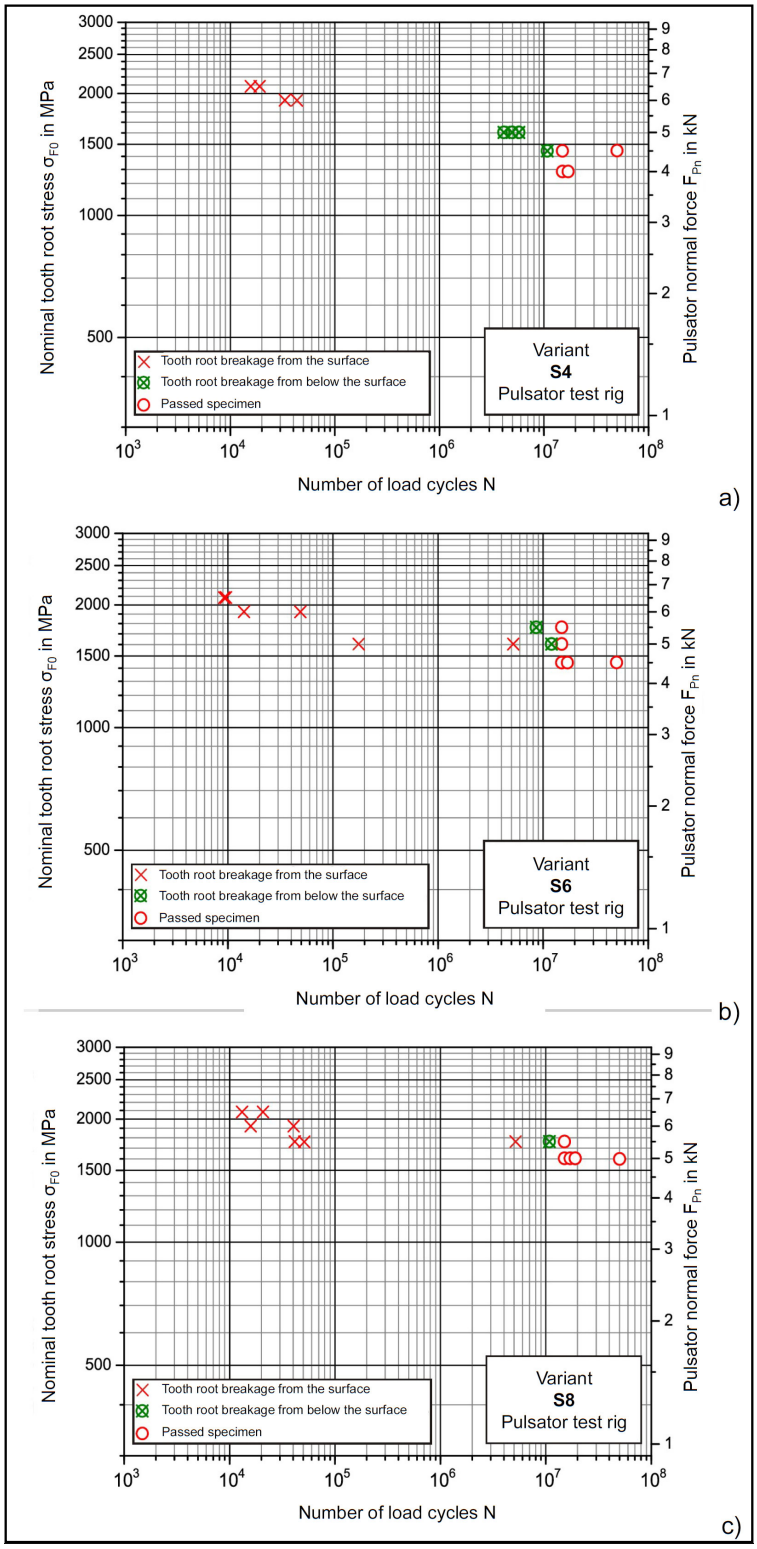

Figure 3 Test results for case-hardened, shot-peened gears on the pulsator test rig of variant a) S4, b) S6 and c) S8 made out of 20MnCr5 (gear data are listed in Table 2) (Ref. 31, translated).

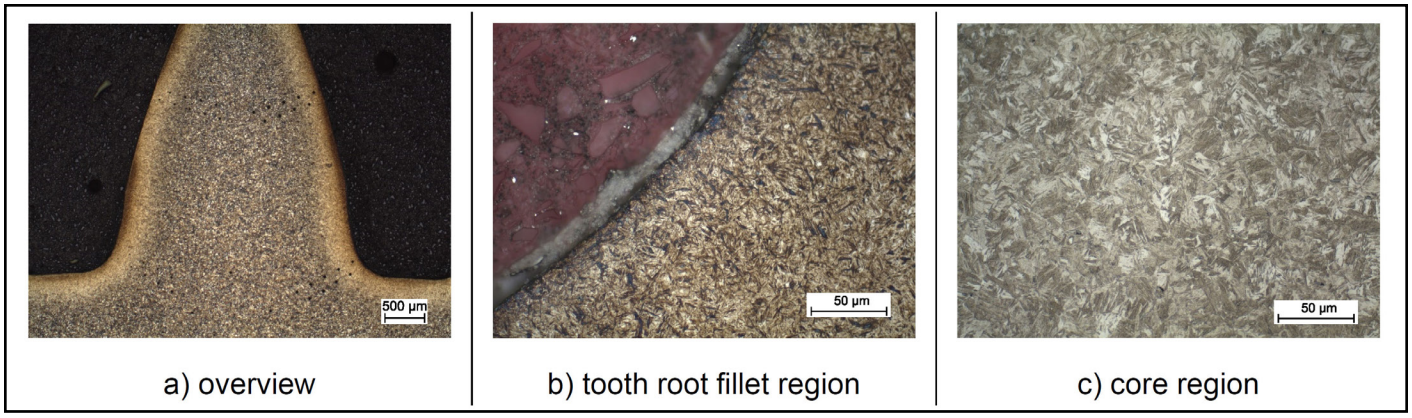

Figure 4 Microstructure of variant S4.

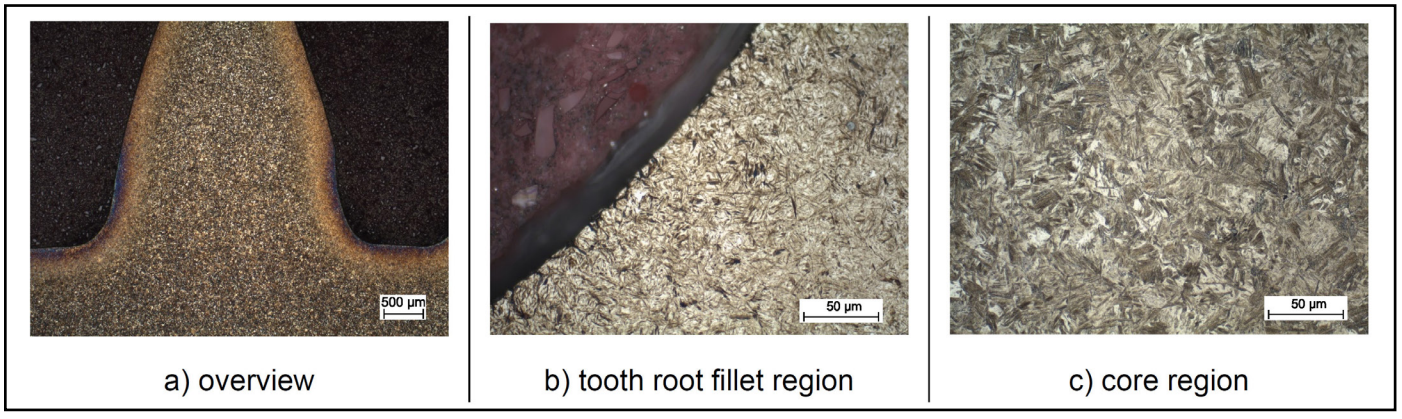

Figure 5 Microstructure of variant S6.

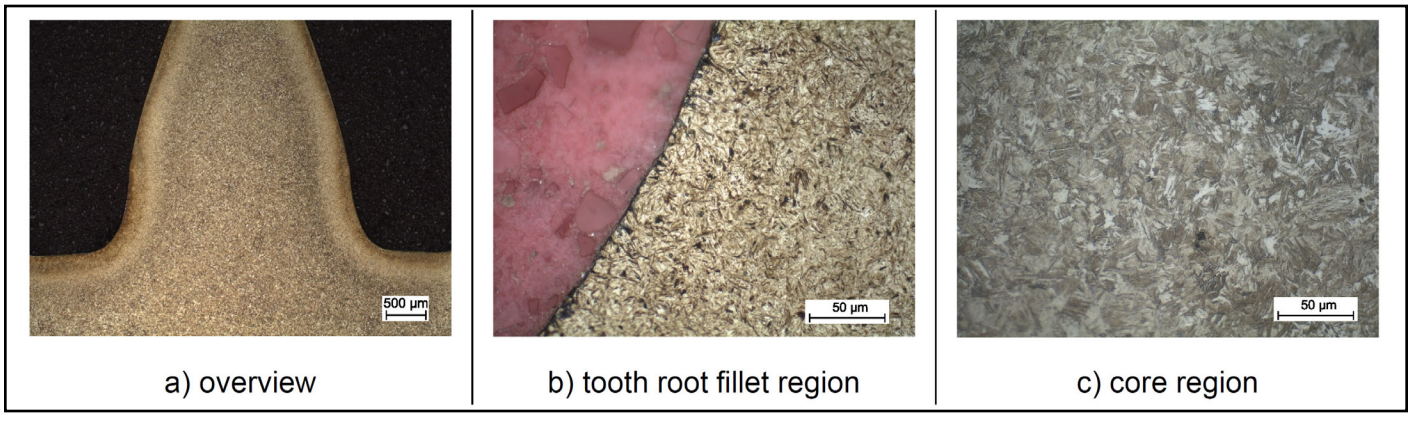

Figure 6 Microstructure of variant S8.

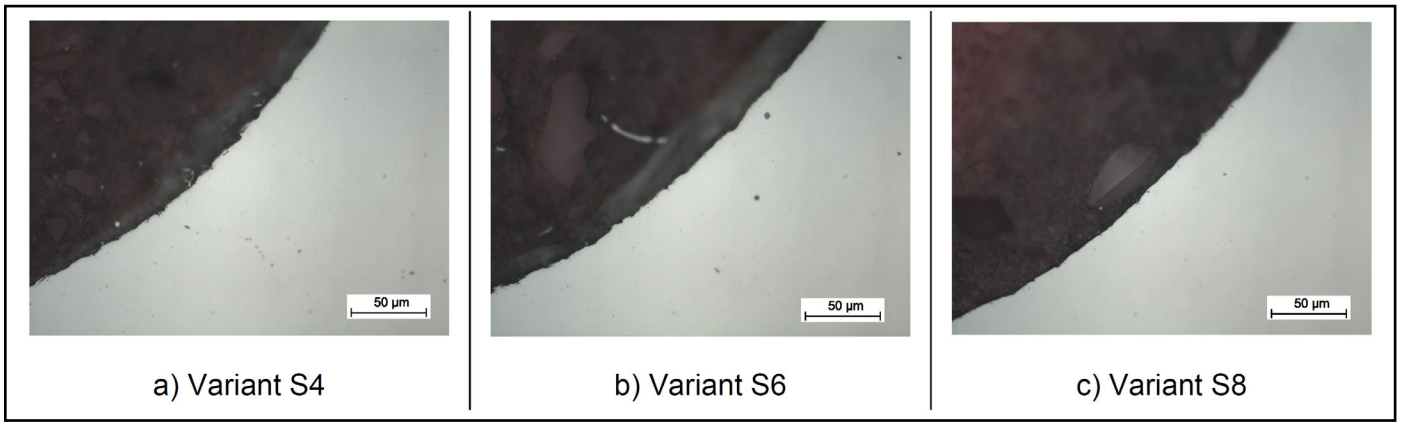

Figure 7 Surface oxidation of variants S4, S6, and S8.

Material and Gear Characterization

In the following, the material and gear characterization of the three investigated variants is presented. The chemical composition of the test variants is listed in Table 5. All three test variants are within the threshold values according to DIN EN ISO 683-3 (Ref. 35). It can be seen that there is a reduced sulfur content, especially in the S6 and S8 variants. These values are well below the threshold value. This measure taken in steel making should prevent the formation of manganese sulfide inclusions. The aluminum content is also lower in the S6 and S8 variants to prevent the formation of aluminum oxide inclusions. However, it should be noted that a certain aluminum content is necessary for fine grain stability. A reduction in aluminum content should therefore not be taken to extremes.

Figures 4–6 show the microstructures of the variants S4, S6 and S8. The microsections for the microstructure are etched with Nital. In each case on the left side, an overview is given, in the center the microstructure in the tooth root fillet, and on the right, the microstructure in the core region is shown. All variants show a smooth transition from the surface layer to the core region with lower and upper bainite in the core region. In the surface layer, variant S4 shows finely dispersed carbides and martensite, variant S6 shows a fine martensitic structure with a low content of retained austenite, and variant S8 also shows a low content of retained austenite and martensite. Figure 7 compares the surface oxidation of all three variants, which is for all variants below 3 µm.

To sum up: All test gears show a microstructure typical for case-hardened gears and no anomalies were visible. In addition, the gears show very low surface oxidation, well below the threshold limits according to ISO 6336, part 5 (Ref. 36).

The dual shot-peening process introduces high residual stresses in the tooth root fillet. Figure 8a confirms high compressive residual stresses at and near the surface. The maximum values range between –1,000 and –1,200 MPa. The dual shot-peening process has an effective depth of about 0.15 to 0.20 mm. All three variants show a maximum for the

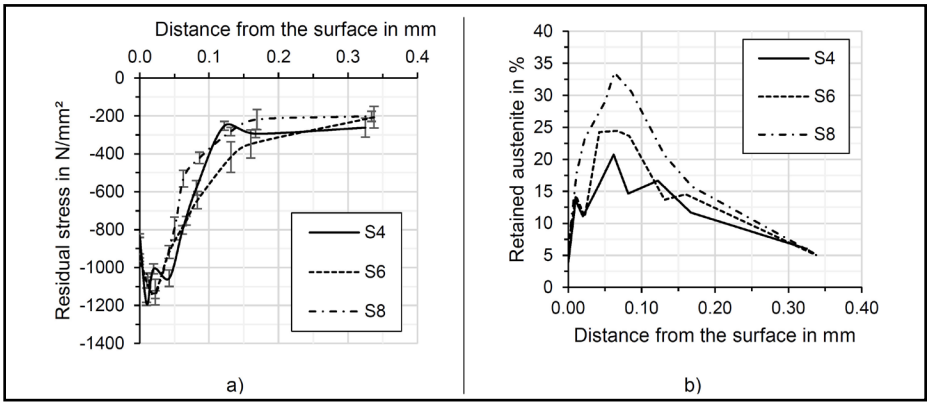

Figure 8 a) Residual stress depth curves in the area of the tooth root fillet and b) retained austenite content in the near-surface area (measured by X-ray diffractometry).

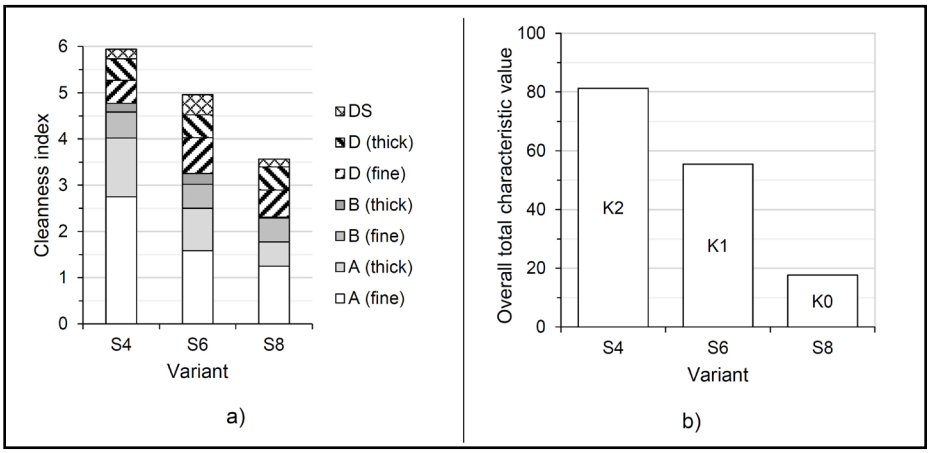

Figure 9 a) Stacked bar diagram of the cleanness indexes according to ISO 4967, method A (Ref. 37) and b) overall total characteristic values according to method K of SEP 1571 (Ref. 38) starting from size class 0 (K0), size class 1 (K1) and size class 2 (K2).

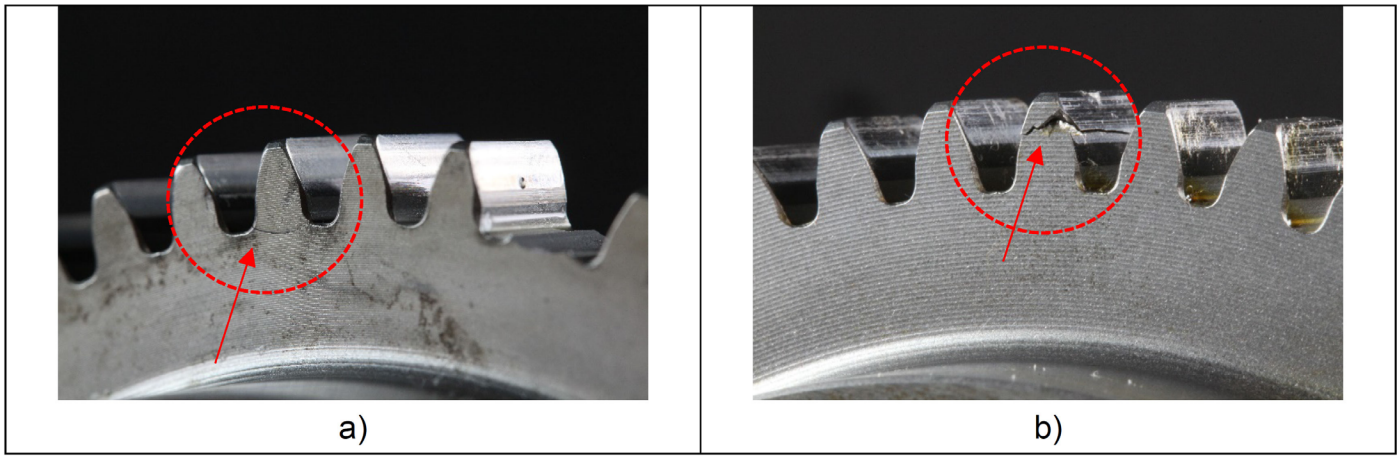

Figure 10 a) Example of a tooth root fracture with crack initiation at or below the surface in the tooth root fillet near the 30° tangent and b) example of a breakage at the tooth flank due to crack initiation at the tooth flank (observed only once each for variant S4 and S6).

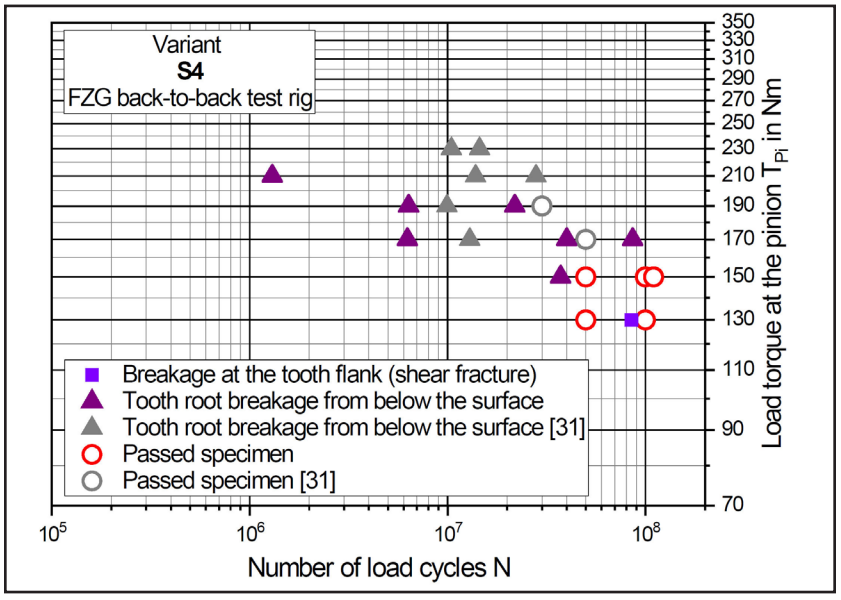

Figure 11 Test results in the range of the endurance limit of variant S4.

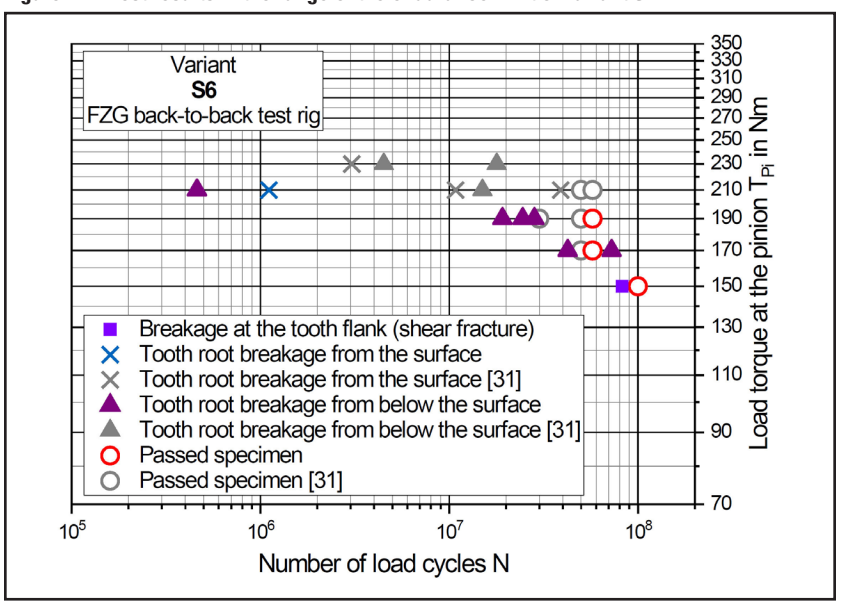

Figure 12 Test results in the range of the endurance limit of variant S6.

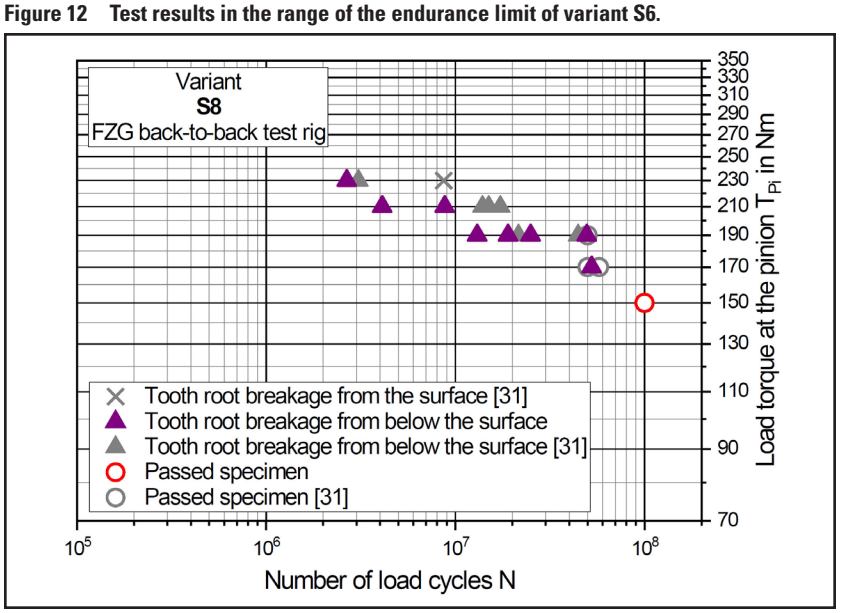

Figure 13 Test results in the range of the endurance limit of variant S8.

retained austenite in a depth range of about 0.05 to 0.10 mm (Figure 8b). Variant S8 shows the highest value for retained austenite, whereas variant S4 shows the lowest value. The nonmetallic inclusions responsible for crack initiation in these variants had a distance from the surface of 0.08 to 0.30 mm. It is thus evident that all inclusions are located behind the compressive residual stress and retained austenite maxima, in the range in which the residual stresses and the retained austenite already decrease again significantly.

Figure 9 gives an overview of the degree of cleanliness. In Figure 9a, the cleanness index for the different inclusion categories according to ISO 4967, method A is shown. Variant S8 shows the best cleanness index, variant S6 lies in between and S4 shows the highest value and therefore the lowest degree of cleanliness. The same tendency can be seen in Figure 9b, according to SEP 1571, method K. The starting size class for method K of SEP 1571 was chosen individually for each variant based on the inclusion content and under consideration of a reasonable effort for the manual evaluation of the degree of cleanliness by a metallographer in industrial practice.

Experimental Investigations of the Tooth Root Bending Strength

Experimental results

In the following, the experimental results on the FZG back-to-back test rig are presented. The tooth flanks of the pinion show slight scrape marks at half tooth height after the test runs. This results from the shortened tip diameter of the wheel. Starting from the scrape mark, some micropitting is visible, which varies in intensity depending on the number of load cycles, the load level, and the variant. Particularly at load cycles above $50 \cdot 10^6$, surface damage on the flank is also evident, which for one test point of variant S4 and variant S6 each was so severe that it initiated a break from the flank (shear fracture); see Figure 10b. All other fractures occurred at the 30° tangent to the tooth root fillet, as Figure 10a illustrates. The crack initiation was hereby either at the surface or from below the surface at a nonmetallic inclusion.

The test points of the investigations on the FZG back-to-back test rig of Schurer (Ref. 31) are colored grey in the following diagrams (Figs. 11–13), whereas the additional test points in the framework of this publication are colored differently. Variant S4 shows passed specimens on the load levels of 130 and 150 Nm up to $100 \cdot 10^6$. At the load level of 170 Nm a specimen reached $50 \cdot 10^6$ load cycles without failure,

whereas one failure due to a crack initiation at a nonmetallic inclusion is even at approximately $75 \cdot 10^6$ load cycles. At the load level of 130 Nm one specimen reached $30 \cdot 10^6$ load cycles. Failures due to a crack initiation at a nonmetallic inclusion are present from a load level of 150 Nm on. At variant S6 a specimen reached $100 \cdot 10^6$ load cycles without failure at a load level of 150 Nm. Further passed specimen are present on the load levels 170, 190 and 210 Nm up to $50 \cdot 10^6$ load cycles. At the load levels of 170 and 190 Nm the gears failed only due to a crack initiation below the surface at a nonmetallic inclusion. The load levels 210 and 230 Nm showed failures from below the surface as well as from the surface. At the load level of 210 Nm a failure due to a crack initiation at the surface is present at approximately $40 \cdot 10^6$ load cycles. Variant S8 shows one passed specimen at $100 \cdot 10^6$ load cycles at a load level of 150 Nm. Only one failure at the load level of 230 Nm is due to a crack initiation at the surface. All other crack initiations are from below the surface at nonmetallic inclusions. Passed specimens at $50 \cdot 10^6$ load cycles are present on the load levels of 170 and 190 Nm. Whereas at the load level of 170 Nm a gear failed due to a crack initiation at a nonmetallic inclusion just above $50 \cdot 10^6$ load cycles.

Crack Area Characteristics

Most of the failures were due to a crack initiation below the surface at a nonmetallic inclusion. Only some of the test gears failed due to a crack initiation at the surface in the tooth root fillet. The crack area characteristic was hereby as typical for surface cracks. No fisheye nor nonmetallic inclusion were present in this case. All tooth root fractures from below the surface showed the typical fisheye characteristic (Fig. 14). The cracks were initiated in all cases at manganese sulfide inclusions. Minor elements of the manganese sulfide inclusions were molybdenum (Mo), magnesium (Mg), aluminum (Al), oxygen (O), and calcium (Ca). The inclusions were either stringer inclusions or oblong shaped.

Discussion and Conclusion

- Based on the experimental studies, the following can be stated:
- All variants show fractures initiated from below the surface at nonmetallic inclusions.
- The fractures from below the surface show a typical fisheye characteristic.
- In the endurance fatigue range, only a few failures from the surface occurred.
- The usual number of load cycles for fractures from below the surface at nonmetallic inclusions is greater than $3 \cdot 10^6$, usually even greater than $10 \cdot 10^6$.
- Relatively fewer tooth root breakages are present above a load cycle number of approximately $50 \cdot 10^6$.

In the following, the experimental investigations on the pulsator test rig from Schurer (Ref. 31) are firstly compared to the extended database on the FZG back-to-back test rig from this publication. Secondly, the experimental database up to $50 \cdot 10^6$ and up to $100 \cdot 10^6$ load cycles is compared and a probable correlation between the experimental results and the degree of cleanliness is checked.

Comparison of the Experimental Investigations on the Pulsator and the Back-to-back Test Rig

In the gear running tests on the back-to-back test rig, 59 teeth are examined simultaneously in one test run. In one test run alone, this corresponds to 2.5 to 3 times the test volume compared to the complete test of the tooth root fatigue strength with the usual assignment of 10 to 12 test points in the pulsator test, in which only two teeth are loaded per test. The probability of a critical nonmetallic inclusion at a critical depth is thus much higher in the course of the gear running tests than in the pulsator tests. In addition, the limiting load cycle number was set on the back-to-back test rig to $100 \cdot 10^6$ (in the pulsator: $15 \cdot 10^6$). Both facts explain why all variants in the gear running tests showed foremost crack initiations below the surface at a nonmetallic inclusion in the endurance fatigue range. When comparing the experimental results, of course, additionally to the presented results, the known systematically differences in gear running tests and pulsator tests should also be kept in mind (Refs. 39, 40) as well as the extended, but still limited available database.

Figure 15a shows the total number of tests failed due to a crack initiation at nonmetallic inclusion in the endurance fatigue range and Figure 15b shows the percentage related to all failed tests. The tooth root fractures of variant S4, with the lowest degree of cleanliness, start on the pulsator and the back-to-back test rig in each case 100 percent below the surface at a nonmetallic inclusion. The

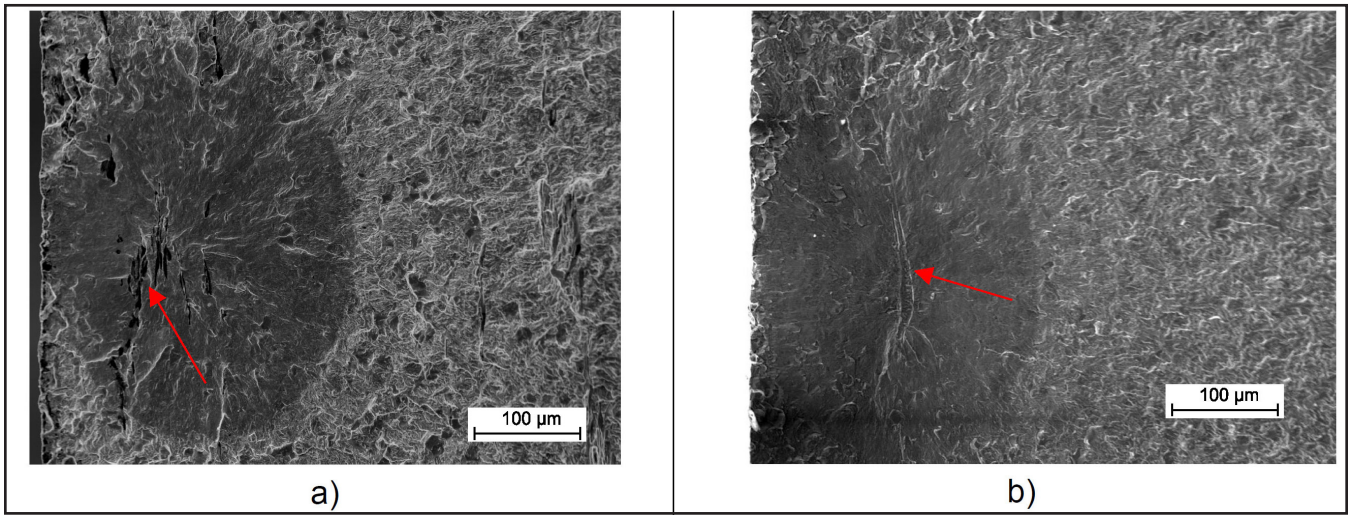

Figure 14 Exemplary a) stringer (variant S4) and b) oblong (variant S8) manganese sulfide inclusion in a fisheye fracture surface.

number of crack initiations below the surface at nonmetallic inclusions for the pulsator tests decreases with a higher degree of cleanliness but not for the gear running tests (see Figure 15a). The greatest difference is present for variant S8.

It can be concluded that the tests on the pulsator test rig with a limiting number of load cycles of $15 \cdot 10^6$ are not fully representative for case-hardened, shot-peened gears made out of steels with a higher degree of cleanliness, and investigations on the back-to-back test rig with a higher number of load cycles could be necessary to determine more reliable results for the tooth root bending strength in the VHCF range.

Comparison of the Experimental Investigations on the Back-to-back Test Rig up to 50 Million and 100 Million Load Cycles

Figure 16 compares the evaluated endurable torque at the pinion for 50 percent failure probability for $50 \cdot 10^6$ and $100 \cdot 10^6$ load cycles. As stated before, the tooth root stress values are deliberately not used for comparison due to the nonlinear relationship between the torque applied to the pinion and the resulting nominal tooth root stress (see Table 4). The endurable torque at the pinion for 50 percent failure probability was determined according to the stair case method (Ref. 41). Hereby, for the evaluation up to $50 \cdot 10^6$ load cycles, all test points, which had load cycles above $50 \cdot 10^6$ load cycles were evaluated as run-outs. The standard deviation was calculated according to the Probit method (Ref. 42).

For all three variants, a further decrease in the load carrying capacity with a higher number of load cycles is observable, especially for variant S6. It can be seen that even up to $100 \cdot 10^6$ load cycles no endurance limit for case-hardened, shot-peened gears can be assumed.

Up to $50 \cdot 10^6$ load cycles, variant S6, which has a degree of cleanliness between variant S4 and S8, shows the highest load carrying capacity. Therefore, with the limited database in Reference 31 and even with the broadened database in the framework of this publication, no proper differentiation between the degree of cleanliness and the tooth root load carrying capacity could be drawn up to $50 \cdot 10^6$ load cycles; compare Figure 16.

However, up to $100 \cdot 10^6$ load cycles and based on the broadened database, a correlation between the degree of cleanliness and the load carrying capacity can be drawn. Variant S4, with the lowest degree of cleanliness, shows the lowest value, whereas variant S8 with the highest degree of cleanliness shows thehighest value. An increase of about 10 percent in load carrying capacity can be stated from variant S4 to variant S8.

It can be concluded that with a higher degree of cleanliness, higher tooth root bending strengths are possible up to the VHCF range.

Summary and Subsequent Steps

The load capacity calculation for gears acc. to standardized methods, like AGMA 2001-D04 (Ref. 1) or ISO 6336 (Ref. 2), are intentionally conservative to ensure broad applicability in industrial practice. However, due to new applications and higher requirements, more detailed design calculations and higher tooth flank and tooth root load carrying capacities up to the very high cycle fatigue (VHCF) range are nowadays often necessary.

For example, with a grid frequency of 50 Hz, two pairs of poles and a speed of 1,500 min^{-1} are required in a wind generator. Common rotor speeds are 14 or 30 min^{-1} and a common gear ratio is 1:100. This results in the gearbox of a wind power plant with an assumed operating time of 30,000 h in approx. $2.7 \cdot 10^9$ loadcycles at the pinion on the input shaft of the transmission (Refs. 43, 44). For an assumed lifetime of 5,000 operating hours of a passenger car and an assumed input speed of the electric motor of 16,000 min^{-1}, load cycles in the range of $4.8 \cdot 10^9$ also result at the pinion on the

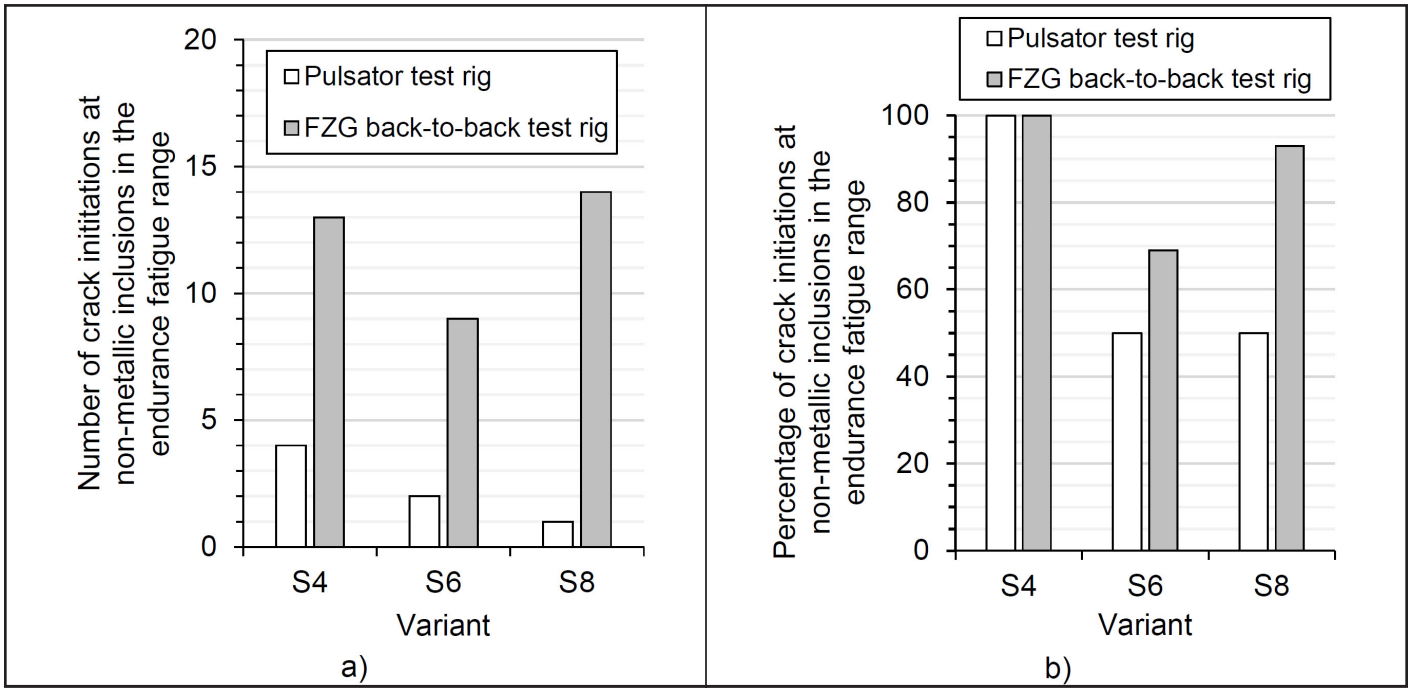

Figure 15 a) Number and b) percentage of crack initiations at nonmetallic inclusions from below the surface in the endurance fatigue range for tests on the pulsator and on the back-to-back test rig (Results of the pulsator tests are shown in Figure 3 and are taken from Reference 31).

input shaft for today's e-mobility transmissionconcepts (Ref 45).

To achieve a higher bending strength in the tooth root area of gears, one approach is to induce increased compressive residual stresses into the stressed area, e.g. by a shot-peening process. The drawback is thatoften there is a change in the crack mechanism. The crack initiation can now occur preferably at nonmetallic inclusions in the steel matrix.

As a result, the working hypothesis of this publication was: the higher the cleanliness the fewer and smallersized the nonmetallic inclusions in the material and therefore the higher the tooth root load carrying capacity of case-hardened, shot-peened gears. This working hypothesis was verified with tests on FZG back-to-back test rigs up to the very high cycle fatigue (VHCF) range (up to $100 \cdot 10^6$ load cycles). The test gear variants were manufactured from steels with a different degree of cleanliness.

The main conclusions of this publication are:

- All variants, even with a high degree of cleanliness (ultra-clean gear steels), show fisheye fractures initiated from below the surface at nonmetallic inclusions and result in a decrease in tooth root bending strength.
- Tests on the pulsator test rig with a limiting number of $15 \cdot 10^6$ load cycles are not fully representative for case-hardened, shot-peened gears made out of steels with a higher degree of cleanliness, due to the limited investigated material volume, and investigations on the back-to-back test rig with a higher number of load cycles could be necessary to determine more reliable results for the tooth root bending strength in the VHCF range.
- With a higher degree of cleanliness, higher tooth root bending strength numbers are possible up to the VHCF range taking into account the different crack mechanism.

The database for the tooth root bending strength between $50 \cdot 10^6$ and $100 \cdot 10^6$ is still very limited on theFZG back-to-back test rig. Therefore, further investigations into gears should concentrate in particular on the range between 50 and 100 million load cycles. In addition, experimental tests above $100 \cdot 10^6$ load cycles should be performed to further expand the database and to check if a second endurance fatigue limit is to be expected at a higher number of load cycles. However, it was also shown that with a higher number of load cycles, damage on the tooth flank can occur and can lead to a fracture. As a result, no tooth root bending strength can be determined. This should be kept in mind when performing such tests with a higher number of load cycles.

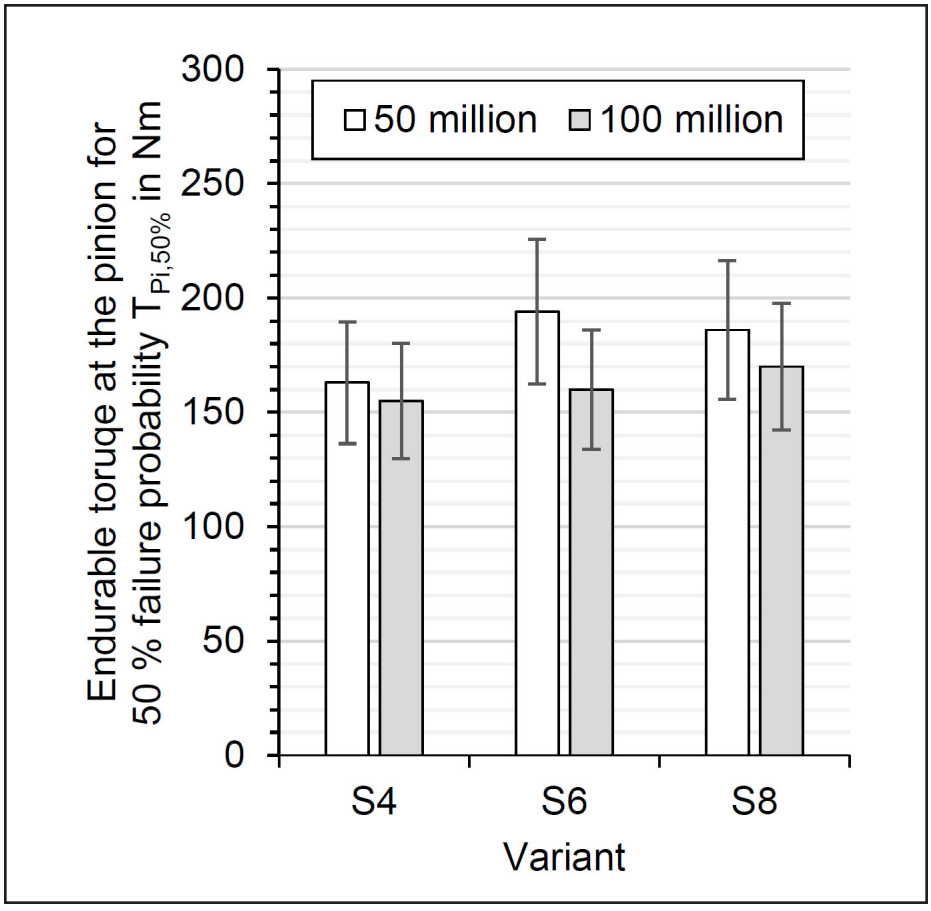

Figure 16 Comparison of the endurable torque at the pinion for 50 % failure probability and standard deviation acc. to the Probit method (Ref. 42) for a limiting number of load cycles of $50 \cdot 10^6$ and $100 \cdot 10^6$.

Furthermore, it has to be noticed that the presented characteristics of a stepwise S-N curve only apply to case-hardened, shot-peened gears with high compressive residual stresses at and close to the surface. For unpeened or shot-blasted case-hardened gears with lower compressive residual stresses, comparableinvestigations prove that the tooth root bending strength is dominated by cracks initiated at the surface andthat these surface cracks typically occur at load cycle numbers below $3 \cdot 10^6$.

Acknowledgment

The underlying research work (Ref. 31) was funded in equal proportions by the "Arbeitsgemeinschaft industrieller Forschungsvereinigungen e.V. (AiF)", the German Federal Ministry of Economics and Technology (BMWi, IGF no. 16662 N) and the "Forschungsvereinigung Antriebstechnik e.V. (FVA)". The results presented in this publication were taken from the FVA research project 293 III "Späte Zahnfußbrüche/ Reinheitsgrad" (Ref. 46). More detailed information on the influence of nonmetallic inclusions is given in the final report.

The underlying research work (Ref. 47) was funded in equal proportions by the "Forschungsvereinigung der Arbeitsgemeinschaft der Eisen und Metall verarbeitenden Industrie e.V. (AVIF)" (A 305 / S 0024/10235/16) and the "Forschungsvereinigung Antriebstechnik e.V. (FVA)". The results presented in this publication were taken from the FVA research project 293 IV "Späte Zahnfußbrüche/ Reinheitsgrad II" (Ref. 47). More detailed information on the influence of nonmetallic inclusions, especially in the very high cycle range, is given in the final report.

References

1. ANSI/AGMA 2001-D04:2004-12. *Fundamental Rating Factors and Calculation Methods for Involute Spur and helical Gear Teeth*.
2. ISO 6336. *Calculation of Load Capacity of Spur and Helical Gears — Part 1–5*.
3. Nishijima, S. u. Kanazawa, K. "Stepwise SN curve and fisheye failure in gigacycle fatigue." *Fatigue Fracture of Engineering Materials and Structures* 22 (1999) 7, S. 601–607. doi: 10.1046/j.1460- 2695.1999.00206.x.
4. Toyoda, T., Kaazawa, T. u. Hisamatus, S. "Influence of inclusions on the fatigue strength of shot peened carburized steel." *Conf Proc: ICSP-5* (1993), S. 333–340.
5. Bathias, C., Drouillac, L. u. Le François, P. "How and why the fatigue S–N curve does not approach a horizontal asymptote." *International Journal of Fatigue* 23 (2001), S. 143–151. doi: 10.1016/S0142- 1123(01)00123-2.
6. Nakajima, M., Kamiya, N., Itoga, H., Tokaji, K. u. Ko, H. "Experimental estimation of crack initiation lives and fatigue limit in subsurface fracture of a high carbon chromium steel." *International Journal of Fatigue* 28 (2006) 11, S. 1540–1546. doi: 10.1016/j.ijfatigue.2005.05.017.
7. Thumser, R., Kleemann, S., Bergmann, J. W. u. Kleemann, A. "Investigation on defect distribution and its statistical evaluation for case hardened material states." *International Journal of Fatigue* 41 (2012), S. 52–56. doi: 10.1016/j.ijfatigue.2012.01.024.
8. Sun, C., Lei, Z., Xie, J. u. Hong, Y. "Effects of inclusion size and stress ratio on fatigue strength for high-strength steels with fish-eye mode failure." *International Journal of Fatigue* 48 (2013), S. 19–27. doi: 10.1016/j.ijfatigue.2012.12.004.
9. Tridello, A., Paolino, D. S., Chiandussi, G. u. Rossetto, M. "VHCF strength decrement in large H13 steel specimens subjected to ESR process." *Procedia Structural Integrity* 2 (2016), S. 1117–1124. doi: 10.1016/j.prostr.2016.06.143.
10. Tridello, A., Paolino, D. S., Chiandussi, G. u. Rossetto, M. "Ultrasonic VHCF tests on AISI H13 steel with two different inclusion content: Assessment of size effects with gaussian specimens." *Procedia Engineering* (2015) 109, S. 121–127. doi: 10.1016/j.proeng.2015.06.218.
11. Tridello, A., Fiocchi, J., Biffi, C. A., Chiandussi, G., Rossetto, M., Tuissi, A. u. Paolino, D. S. "VHCF response of heat-treated SLM Ti6Al4V Gaussian specimens with large loaded volume." *Procedia Structural Integrity* 18 (2019), S. 314–321. doi: 10.1016/j.prostr.2019.08.171.
12. Sandaiji, Y. u. Tamura, E. "Influence of loading type on fracture behaviour of high strength steel under very high cycle fatigue." In: Zimmermann, M. u. Christ, H.-J. (Hrsg.): *VHCF7. Seventh International Conference on Very High Cycle Fatigue*: July 3–5, 2017, Dresden, Germany. Siegener Werkstoffkundliche Berichte, 14/2017. Siegen: Siegener Werkstoffkundliche Berichte 2017, S. 25–30.
13. Nambu, K. u. Egami, N. "Influence of hybrid surface modification on very high cycle fatigue strength of various steel materials." In: Zimmermann, M. u. Christ, H.-J. (Hrsg.): *VHCF7. Seventh International Conference on Very High Cycle Fatigue*: July 3–5, 2017, Dresden, Germany. Siegener Werkstoffkundliche Berichte, 14/2017. Siegen: Siegener Werkstoffkundliche Berichte 2017, S. 302–307.
14. Wang, Q., Bathias, C., Kawagoishi N. u. Chen Q. "Effect of inclusion on subsurface crack initiation and gigacycle fatigue strength." *International Journal of Fatigue* 24 (2002) 12, S. 1269–1274. doi: 10.1016/S0142-1123(02)00037-3.
15. Tallerico, T. F. u. Cameron, Z. A. *Ultrasonic Gear Steel Fatigue at NASA*. Anaheim, CA 2019.
16. Zhao, A., Xie, J., Sun, C., Lei, Z. u. Hong, Y. "Effects of strength level and loading frequency on very-high-cycle fatigue behavior for a bearing steel." *International Journal of Fatigue* 38 (2012),S. 46–56. doi: 10.1016/j.ijfatigue.2011.11.014.
17. Zhang, J. W., Lu, L. T., Shiozawa, K., Zhou, W. N. u. Zhang, W. H. "Effect of nitrocarburizing and post-oxidation on fatigue behavior of 35CrMo alloy steel in very high cycle fatigue regime." *International Journal of Fatigue* 33 (2011) 7, S. 880–886. doi: 10.1016/j.ijfatigue.2011.01.016
18. Zammit A., Mhaede M., Grech M., Abela S. u. Wagner L. "Influence of shot peening on the fatigue life of Cu–Ni austempered ductile iron." *Materials Science and Engineering: A* (2012) 545, S. 78–85. doi: 10.1016/j.msea.2012.02.092.
19. Torabian, N., Favier, V., Dirrenberger, J., Adamski, F., Ziaei-Rad, S. u. Ranc, N. "Investigation of the response of dual-phase steels submitted to 20KHz and low frequency fatigue loadings." In: Zimmermann, M. u. Christ, H.-J. (Hrsg.): *VHCF7. Seventh International Conference on Very High Cycle Fatigue*: July 3–5, 2017, Dresden, Germany. Siegener Werkstoffkundliche Berichte, 14/2017. Siegen: Siegener Werkstoffkundliche Berichte 2017, S. 368–373.
20. Zhu, M.-L., Xuan, F.-Z., Du, Y.-N. u. Tu, S.-T. "Very high cycle fatigue behavior of a low strength welded joint at moderate temperature." *International Journal of Fatigue* 40 (2012), S. 74–83. doi: 10.1016/j.ijfatigue.2012.01.014.
21. Murakami, Y., Yokoyama, N. N. u. Nagata, J. "Mechanism of fatigue failure in ultralong life regime." *Fatigue Fracture of Engineering Materials and Structures* 25 (2002) 8–9, S. 735–746. doi: 10.1046/j.1460-2695.2002.00576.x.
22. Murakami, Y., Nomoto, T. u. Ueda, T. "Factors influencing the mechanism of superlong fatigue failure in steels." *Fatigue Fracture of Engineering Materials and Structures* 22 (1999) 7, S. 581–590. doi: 10.1046/j.1460-2695.1999.00187.x.
23. Mughrabi, H. "On the life controlling microstructural fatigue mechanisms in ductile metals and alloys in the gigacycle regime." *Fatigue Fracture of Engineering Materials and Structures* 22 (1999) 7, S. 633–641. doi: 10.1046/j.1460-2695.1999.00186.x.
24. Mughrabi, H. "On 'multi-stage' fatigue life diagrams and the relevant life-controlling mechanisms in ultra high-cycle fatigue." *Fatigue Fracture of Engineering Materials and Structures* 25 (2002) 8–9, S. 755–764. doi: 10.1046/j.1460-2695.2002.00550.x.
25. Bathias, C. "Fatigue Limit." In: Wang, Q. J. u. Chung, Y.-W. (Hrsg.): *Encyclopedia of Tribology*. Boston, MA: Springer US 2013, S. 1041–1052.
26. Bretl, N. T. "Einflüsse auf die Zahnfußtragfähigkeit einsatzgehärteter Zahnräder im Bereich hoher Lastspielzahlen [eng.: influences on the tooth root load carrying capacity of case-hardened gears in the range of high load cycles]," Technical University of Munich Dissertation. Munich 2010.
27. Stenico, A. "Werkstoffmechanische Untersuchungen zur Zahnfußtragfähigkeit einsatzgehärteter Zahnräder [eng.: material-mechanical investigations of the tooth root load carrying capacity of case- hardened gears]," Technical University of Munich Dissertation. Munich 2007.
28. Stenico, A., Krug, T., Oster, P., Lang, K.-H., Höhn, B.-R. u. Löhe, D. "Eigenspannungen Zahnfuß. Eigenspannungseinfluss auf die Zahnfußtragfähigkeit kleinmoduliger Zahnräder," FVA 369 I+II. FVA-Heft Nr. 745, Frankfurt a. M. 2004.
29. Bretl, N. T., Tobie, T. u. Höhn, B.-R. "Einflüsse auf die Zahnfußtragfähigkeit einsatzgehärteter Zahnräder im Bereich hoher Lastspielzahlen [eng.: Influences on the tooth root load carrying capacity of case-hardened gears in the range of high load cycles]," FVA project 293 II. FVA issue 851 Nr. 851, Frankfurt on the Main, Germany 2008.
30. Bretl N., Schurer, S., Tobie, T., Stahl, K. u. Höhn, B.-R. "Investigations on Tooth Root Bending Strength of Case Hardened Gears in the Range of High Cycle Fatigue." AGMA Technical Paper 13FTM09 (2013).
31. Schurer, S. "Einfluss nichtmetallischer Einschlüsse in hochreinen Werkstoffen auf die Zahnfußtragfähigkeit [eng.: influence of nonmetallic inclusions in ultra-clean materials on the tooth root load-carrying capacity]," Technical University of Munich Dissertation. Munich 2016.
32. Winkler, K. J., Schurer, S., Tobie, T. u. Stahl, K. "Investigations on the tooth root bending strength and the fatigue fracture characteristics of case-carburized and shot-peened gears of different sizes." *Proceedings of the Institution of Mechanical Engineers, Part C: Journal of Mechanical Engineering Science* (2019). doi: 10.1177/0954406219841650.
33. Fuchs, D., Schurer, S., Tobie, T. u. Stahl, K. "On the determination of the bending fatigue strength in and above the very high cycle fatigue regime of shot-peened gears." *Forschung im Ingenieurwesen* (2021). doi: 10.1007/s10010-021-00499-2.
34. Thoma, F., Otto, M. u. Höhn, B.-R. "RIKOR I - Erweiterung Ritzelkorrekturprogramm (RIKOR) zur Bestimmung der Lastverteilung von Stirnradgetrieben [eng.: RIKOR I - Extension of the pinion correction program (RIKOR) to determine the load distribution of the gears," FVA 30 VI. FVA-Heft Nr. 914, Frankfurt a. M. 2009.
35. *DIN EN ISO 683-3:2019*. "Für eine Wärmebehandlung bestimmte Stähle, legierte Stähle und Automatenstähle - Teil 3: Einsatzstähle. Heat-treatable steels, alloy steels and free-cutting steels -Part 3: Case-hardening steels."
36. *ISO 6336-5:2016*. "Calculation of load capacity of spur and helical gears - part 5: strength and quality of materials."
37. *ISO 4967:2013*. "Steel - Determination of content of nonmetallic inclusions - Micrographic method using standard diagrams."
38. *SEP 1571-2:2017-08*. "Bewertung von Einschlüssen in Edelstählen auf Basis der Einschlussflächen -Teil 2: Verfahren K und M."
39. H. Rettig. "Ermittlung von Zahnfußfestigkeit-Kennwerten auf Verspannungsprüfständen und Pulsatoren." *Antriebstechnik* 26 (1987) 2, S. 51–55.
40. McPherson, D. R. u. Rao, S. B. "Methodology for Translating Single Tooth Bending Fatigue Data to be Comparable to Running Gear Data." *Gear Technology* March/April 2008 (2008), S. 42–51.
41. Hück, M. *Ein verbessertes Verfahren für die Auswertung von Treppenstufenversuchen* (1983).
42. Hösel, T. u. Joachim, F. "Zahnflankenwälzfestigkeit unter Berücksichtigung der

Ausfallwahrscheinlichkeit." *Antriebstechnik* 17 (1978) 12, S. 533–537.
43. Gesamtverband der deutschen Versicherungswirtschaft: Erneuerbare Energien 2017.
44. HBM an HBK company: "Drehmomentmessung in Windenergieanlagen - heute so aktuell wie damals, 2021." *www.hbm.com/de/3108/drehmomentmessung-in-windenergieanlagen/* , abgerufen am: 02.09.2021.
45. Industrie Magazin: Wiener Motorensymposium: Autos werden für 5.000 Betriebsstunden gebaut, 2020. *https://industriemagazin.at/a/wiener-motorensymposium-autos-werden-fuer-5000-betriebsstunden-gebaut*, abgerufen am: 02.09.2021.
46. Schurer, S., Tobie, T. u. Stahl, K. "Tragfähigkeitsgewinn im Zahnfuß durch hochreine Stähle [eng.: load carrying capacity increase in the tooth root due to ultra-clean steels]," FVA research project 293 III. FVA issue 1148 Nr. 1148, Frankfurt on the Main, Germany 2015.
47. Fuchs, D., Tobie, T. u. Stahl, K. "Untersuchungen zum Fehlstellenversagen an Zahnrädern und deren Einfluss auf die Zahnradtragfähigkeit [eng.: Investigations into the defect failure of gears and its influence on the gear load carrying capacity," FVA research project 293 IV, Frankfurt on the Main, Germany 2021.

For Related Articles Search
shot peening
at www.geartechnology.com

Daniel Fuchs studied (2011–2016) at: Ostbayerische Technische Hochschule Regensburg (OTH Regensburg), Germany. Since 2016 he has served as a research associate at the Institute of Machine Elements — Gear Research Centre (FZG) of the Technical University of Munich. Fuchs' expertise is in the influence of nonmetallic inclusions on the tooth root load carrying capacity of gears and the influence of coarse grain on the load carrying capacity of gears.

Dr.-Ing. Thomas Tobie is head of the department "Load Carrying Capacity of Cylindrical Gears" at the Gear Research Center (FZG), Technical University of Munich. He is specialized in the fields of gear materials, heat treatment, gear lubricants, gear strength and gear testing with focus on all relevant gear failure modes like tooth root fracture, pitting, micro-pitting, scuffing and wear as well as subsurface initiated fatigue failures. Dr. Tobie an active member of several national and international working groups of DIN, ISO, IEC and CEC and author of numerous papers at scientific journals and conferences.

Prof. Dr.-Ing. Karsten Stahl is full professor at the Institute for Machine Elements and director of Gear Research Center (FZG) at the Technical University Munich. FZG research focuses on experimental and analytical investigations of endurance, tribology, NVH, materials and fatigue life analysis on gears, transmission components and drive systems. Prof. Stahl is board member of several scientific associations, convener of DIN and ISO working groups, editor of several scientific journals, author of several hundred publications, and president of the International Conference on Gears.